Catalysis Letters Vol. 106, Nos. 1–2, January 2006 (© 2006)
DOI: 10.1007/s10562-005-9196-1

Catalytic performance of the Sb–V mixed oxide on Sb–V–O/SiO_2 catalysts in methane selective oxidation to formaldehyde

Haidong Zhang, Jing Zhang, Keqiang Sun, Zhaochi Feng, Pinliang Ying, and Can Li*

State Key Laboratory of Catalysis, Dalian Institute of Chemical Physics, Chinese Academy of Sciences, P. O. Box 110, Dalian, 116023, China

Received 23 July 2005; accepted 7 October 2005

Sb–V–O/SiO_2 catalysts were prepared and investigated in methane selective oxidation with O_2 as oxidant. Sb–V–O/SiO_2 catalysts are active and selective in methane selective oxidation. The formaldehyde yield obtained on Sb–V–O/SiO_2 catalysts is clearly higher than that for VO_X/SiO_2 and SbO_X/SiO_2 catalysts. A one-pass formaldehyde yield up to 3% was obtained on Sb–V–O/SiO_2 catalysts at 650 °C. XRD and UV Raman studies showed that the phase of Sb–V mixed oxide on Sb–V–O/SiO_2 catalysts transformed with decreasing Sb/V ratio from Sb_2VO_5 to $SbVO_4/VSb_{1\text{-}X}O_{4\text{-}1.5X}$ phase. The Sb–V mixed oxide in Sb_2VO_5 phase is more active and selective than that in $SbVO_4/VSb_{1\text{-}X}O_{4\text{-}1.5X}$ phase.

KEY WORDS: methane; selective oxidation; formaldehyde; antimony–vanadium mixed oxide; phase transform.

1. Introduction

Methane selective oxidation with O_2 as oxidant to methanol or formaldehyde has been paid much attention in the past decades and still remains as a great challenge in catalysis [1–4]. Many supported single metal oxide or multi-component metal oxide catalysts have been widely studied in this reaction [4–15]. It was found that silica-supported vanadium and molybdenum oxide catalysts were more effective than other catalysts [8–11]. However, the formaldehyde selectivity for either vanadium or molybdenum catalysts drops dramatically with increasing methane conversion and nearly no C_1-oxygenates can be obtained at methane conversion higher than 20% under atmospheric pressure without radical initiator [8]. Searching for more selective catalysts is always crucial for this study. In our previous work [16], it was found that SbO_X/SiO_2 catalysts can be used to catalyze methane selective oxidation with O_2 as oxidant under atmospheric pressure and the formaldehyde selectivity for SbO_X/SiO_2 catalysts does not drop sharply with increasing methane conversion. The one-pass formaldehyde yield obtained on SbO_X/SiO_2 catalysts is similar to that for MoO_X/SiO_2 catalysts tested under same conditions [16]. However, SbO_X/SiO_2 catalysts are less active than vanadium oxide or molybdenum oxide catalysts. It is difficult to achieve high one-pass formaldehyde yield on SbO_X/SiO_2 catalysts because of their relatively low activity.

We know that, in the methane selective oxidation with O_2 as oxidant, vanadium oxide catalysts are more active than molybdenum oxide catalysts under same conditions and the formaldehyde yield obtained on vanadium oxide catalysts are generally higher than that for molybdenum oxide catalysts [12,13,15]. It is possible to achieve high methane conversion with remarkable formaldehyde selectivity by combinational use of antimony and vanadium oxides. In the present work, three different series of silica supported Sb–V mixed oxide catalysts (Sb–V–O/SiO_2) were prepared and investigated in methane selective oxidation with O_2 as oxidant under atmospheric pressure. At same time, some silica supported vanadium oxide catalysts (VO_X/SiO_2) were also prepared and tested as comparisons. It is found that the Sb–V mixed oxides dispersed on silica show both high methane conversion and high formaldehyde selectivity. Higher one-pass formaldehyde yield can thus be obtained for Sb–V–O/SiO_2 catalysts than that for either VO_X/SiO_2 or SbO_X/SiO_2 catalysts.

2. Experimental

Three series of Sb–V–O/SiO_2 catalysts labeled as $Sb_5V_{0.14\text{–}2.8}O/SiO_2$, $Sb_{10}V_{0.28\text{–}5.6}O/SiO_2$ and $Sb_{20}V_{0.56\text{–}11.2}O/SiO_2$ (the subscript numbers mean the loading of Sb_2O_5 and V_2O_5) were prepared with Sb_2O_5 loadings at 5, 10 and 20 wt%, respectively. SbO_X and VO_X concentrations were estimated based on Sb_2O_5 and V_2O_5 loadings. V_2O_5 loading varies in the range of Sb/V ratio, 1/1, 1/2, 1/5, 1/10 and 1/20. Sb–V–O/SiO_2 catalysts were prepared by a two-step impregnation method. At first, silica (391 $m^2\ g^{-1}$) was impregnated with $SbCl_5$ (Acros)-ethanol solution. The impregnates were dried at room temperature and then impregnated again with aqueous solution of NH_4VO_3 (Acros). Aqueous ammonia solution was then used to adjust the pH value of the

---

* To whom correspondence should be addressed.
E-mail: canli@dicp.ac.cn

impregnates to 8–9. VO_X/SiO_2 catalysts were prepared by the impregnation of silica with aqueous solution of NH_4VO_3. All solid products were dried at 120 °C and then calcined in air at 700 °C for 4 h. Methane selective oxidation was performed in a microreactor system under atmospheric pressure, using O_2 as oxidant. An Agilent 6890N GC with FID and TCD was employed to do on-line analysis of products. Methane conversion and formaldehyde selectivity were calculated using an external standard method based on following equations:

$$CH_4\text{conversion} = (M_{CH_4,in} - M_{CH_4,out})/M_{CH_4,in} \times 100\%$$

$$\text{HCHO selectivity} = M_{HCHO}/(M_{CH_4,in} - M_{CH_4,out}) \times 100\%$$

where M_{CH_4}, *in* and M_{CH_4}, *out* are the amount (mol) of methane feed in and remaining in the effluent; M_{HCHO} is the amount (mol) of formaldehyde detected.

X-ray diffraction measurements were performed on a Rigaku D/max-2500/PC X-ray diffractometer with Cu–Kα radiation (50 kV, 250 mA) from 15 to 70° at a 5°/min scan speed. UV Raman spectra were recorded on a Jobin-Yvon T64000 Raman spectrograph using 325 nm line of a He–Cd laser with 25 mW output as the excitation source.

3. Results and discussion

Figure 1 gives methane conversion and formaldehyde selectivity for $Sb_5V_{0.14-2.8}O/SiO_2$, $Sb_{10}V_{0.28--5.6}O/SiO_2$ and $Sb_{20}V_{0.56-11.2}O/SiO_2$ catalysts at 650 °C. Methane conversion for Sb–V–O/SiO_2 catalysts is much higher than that for SbO_X/SiO_2 catalysts tested under same conditions [16]. The formaldehyde selectivity for Sb–V–O/SiO_2 catalysts decreases with V_2O_5 loading but the formaldehyde selectivity higher than 10% can still be achieved while methane conversion is higher than 20%. For $Sb_5V_{1.4}O/SiO_2$ catalyst, 23.8% methane conversion can be obtained with 11.0% HCHO selectivity. For $Sb_{10}V_{1.12}O/SiO_2$ catalyst, 15.0% methane conversion can be obtained with 15.5% formaldehyde selectivity. Thus one-pass formaldehyde yield at 2.6% (for $Sb_5V_{1.4}O/SiO_2$) and 2.5% (for $Sb_{10}V_{1.12}O/SiO_2$) can be achieved, respectively.

Figure 2 shows one-pass formaldehyde yield for 5 wt% Sb_2O_5/SiO_2, VO_X/SiO_2 (0.56, 1.12 and 1.4 wt%), $Sb_5V_{0.56}O/SiO_2$, $Sb_5V_{1.4}O/SiO_2$ and $Sb_{10}V_{1.12}O/SiO_2$ catalysts at different temperatures. 5 wt% Sb_2O_5/SiO_2 catalyst shows the highest formaldehyde yield among 1–20 wt% SbO_X/SiO_2 catalysts [16] but the formaldehyde yield for 5 wt% Sb_2O_5/SiO_2 catalyst is much lower than that for VO_X/SiO_2 catalysts. The formaldehyde yield for VO_X/SiO_2 catalysts increases with increasing V_2O_5 loading and reaches its maximum (1.6%) while V_2O_5 loading is 1.12 wt% then drops with further increasing V_2O_5 loading. This formaldehyde yield value is very close to the typical results obtained on vanadium oxide catalysts in recent reports [5,9]. It can be seen that the combinational use of antimony and vanadium components evidently enhances formaldehyde yield and the increment of formaldehyde yield, comparing with VO_X/

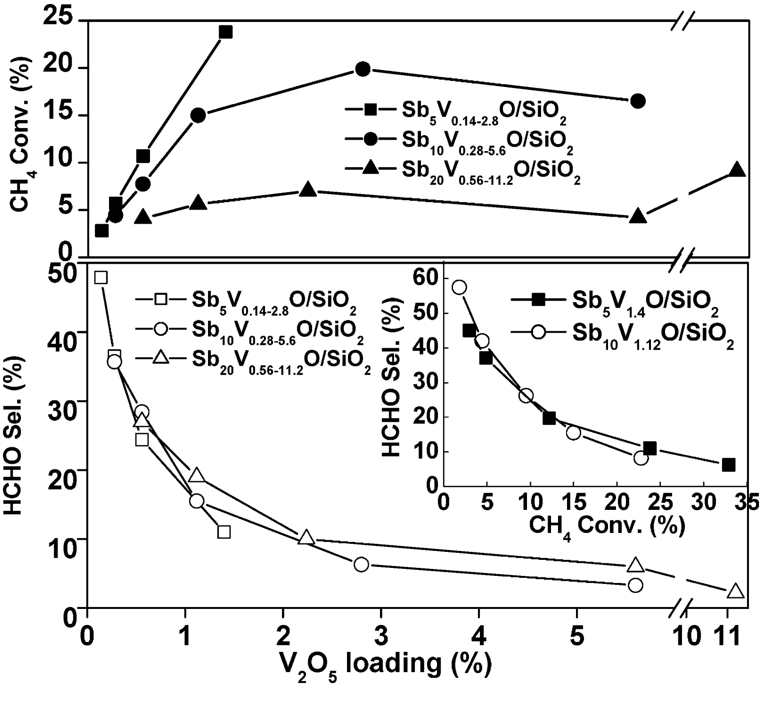

Figure 1. CH_4 conversion and HCHO selectivity for $Sb_5V_{0.14-2.8}O/SiO_2$, $Sb_{10}V_{0.28-5.6}O/SiO_2$ and $Sb_{20}V_{0.56-11.2}O/SiO_2$ catalysts at 650 °C; the inset is the HCHO selectivity for $Sb_{10}V_{1.12}O/SiO_2$ and $Sb_5V_{1.4}O/SiO_2$ catalysts as a function of CH_4 conversion. (0.2 g catalyst, total flow rate 0.07 mol (STY) h^{-1}, $CH_4/O_2/He = 2/1/7$)

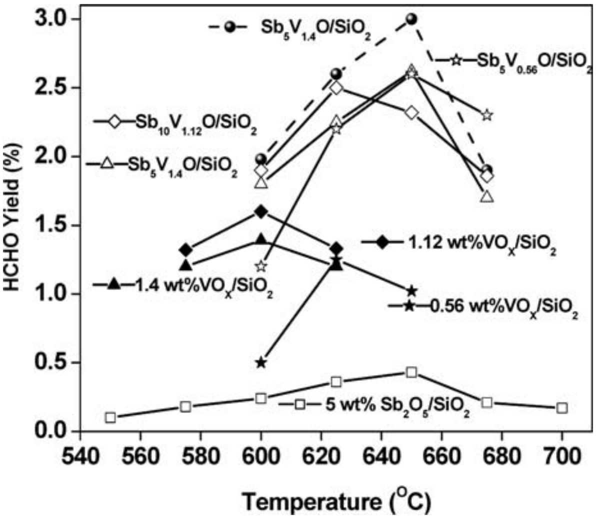

Figure 2. One pass HCHO yield in MSO. Solid lines: Sb_2O_5/SiO_2 (5 wt%), VO_X/SiO_2(0.56, 1.12 and 1.4 wt%), $Sb_5V_{0.56}O/SiO_2$, $Sb_5V_{1.4}O/SiO_2$ and $Sb_{10}V_{1.12}O/SiO_2$ catalysts (0.2 g catalyst, total flow rate 0.07 mol (STY) h^{-1}, $CH_4/O_2/He = 2/1/7$); dashed line: one pass HCHO yield for $Sb_5V_{1.4}O/SiO_2$ catalyst (0.2 g catalyst, total flow rate 0.09 mol (STY) h^{-1}, $CH_4/O_2/He = 2/1/11$).

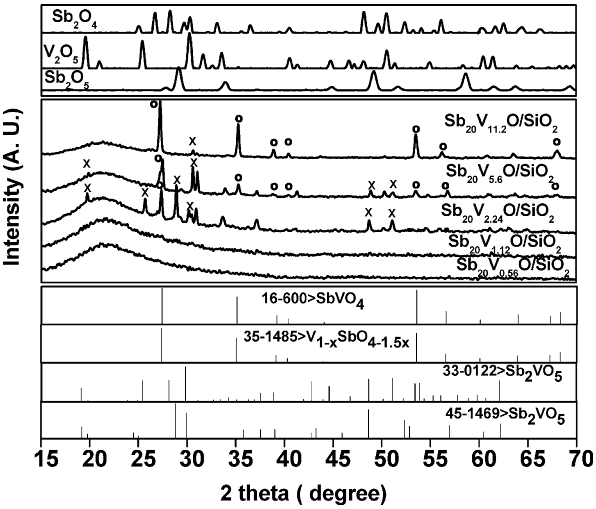

Figure 3. XRD patterns of V_2O_5, Sb_2O_4, Sb_2O_5, and $Sb_{20}V_{0.56-11.2}O/SiO_2$ catalysts. (×: Sb_2VO_5; o: $SbVO_4/VSb_{1-X}O_{4-1.5X}$).

SiO_2 catalysts, is in the range of 50–150%. The formaldehyde yield up to 2.6% can be achieved on $Sb_5V_{1.4}O/SiO_2$ and $Sb_5V_{0.56}O/SiO_2$ catalysts. A formaldehyde yield up to 3.0% can be achieved on $Sb_5V_{1.4}O/SiO_2$ at 650 °C when total flow increases to 0.09 mol (STY) h^{-1}. This formaldehyde yield obtained on Sb–V–O/SiO_2 catalysts is higher than recent results for single metal oxide catalysts such as molybdenum oxide [15] and vanadium oxide [5,9] catalysts.

In figure 1, we also can see that the methane conversion for $Sb_5V_{0.14-2.8}O/SiO_2$ catalysts increase but the formaldehyde selectivity decreases with V_2O_5 loading. This trend for $Sb_5V_{0.14-2.8}O/SiO_2$ catalysts is similar to that for other catalysts in methane selective oxidation, e.g., molybdenum oxide and vanadium oxide catalysts. Differently, methane conversion for $Sb_{10}V_{0.28-5.6}O/SiO_2$ catalysts increases with V_2O_5 loading at first but decreases while V_2O_5 loading reaches 5.6 wt%. The methane conversion for $Sb_{20}V_{0.56-11.2}O/SiO_2$ catalysts increases with V_2O_5 loading and drops sharply while V_2O_5 loading reaches 5.6 wt% and then increases again. At the same time, formaldehyde selectivity for $Sb_{10}V_{5.6}O/SiO_2$ and $Sb_{20}V_{0.56-11.2}O/SiO_2$ catalysts decrease with increasing V_2O_5 loading. It can be inferred from the catalytic performance of $Sb_{10}V_{0.28-5.6}O/SiO_2$ and $Sb_{20}V_{0.56-11.2}O/SiO_2$ catalysts that a change of active species over these catalysts takes place while V_2O_5 loading is about 5.6 wt%.

Figure 3 gives the XRD patterns of V_2O_5, Sb_2O_4, Sb_2O_5, and $Sb_{20}V_{0.56-11.2}O/SiO_2$ catalysts. No diffraction peak of bulk V_2O_5, Sb_2O_4 or Sb_2O_5 can be observed in the patterns of $Sb_{20}V_{0.56-11.2}O/SiO_2$ catalysts. This is agreed with the fact that no diffraction peak of bulk Sb_2O_5, Sb_2O_4 or Sb_2O_3 can be observed in the XRD patterns of Sb_2O_5/SiO_2 catalysts prepared from $SbCl_5$ even the loading of Sb_2O_5 reaches 20 wt% [16]. In the pattern of $Sb_{20}V_{2.24}O/SiO_2$ catalyst, the characteristic peaks of Sb–V mixed oxide in Sb_2VO_5 phase at 19.2°, 25.4°, 28.1°, 29.8°, 48.7° and 51.1° can be observed. These diffraction peaks become very weak when V_2O_5 loading increases to 5.6 wt% and disappear when V_2O_5 loading reaches 11.2 wt%. The characteristic peaks of Sb–V mixed oxide in $SbVO_4/VSb_{1-X}O_{4-1.5X}$ phase at 27.3°, 35°, 39.2°, 40.4°, 53.5°, 56.5° and 68.3° can be observed in the XRD patterns of $Sb_{20}V_{5.6}O/SiO_2$ and $Sb_{20}V_{11.2}O/SiO_2$ catalysts. We can know from XRD results that, on $Sb_{20}V_{0.56-11.2}O/SiO_2$ catalysts, antimony and vanadium component are mainly in Sb–V mixed oxide and a phase transform of Sb–V mixed oxide from Sb_2VO_5 to $SbVO_4/VSb_{1-X}O_{4-1.5X}$ phase takes place while V_2O_5 loading reaches 5.6 wt%. This may be the reason for the drop of methane conversion for $Sb_{20}V_{0.56-11.2}O/SiO_2$ catalysts while V_2O_5 loading reaches 5.6 wt%. The Sb–V mixed oxide in Sb_2VO_5 phase is more active and selective in methane selective oxidation than $SbVO_4/VSb_{1-X}O_{4-1.5X}$ phase.

Figure 4 shows the UV Raman spectra of V_2O_5, Sb_2O_4, Sb_2O_5 and $Sb_{20}V_{0.56-11.2}O/SiO_2$ catalysts. In the spectra of $Sb_{20}V_{0.56-11.2}O/SiO_2$ catalysts, we can see four bands at 190, 260, 400 and 460 cm^{-1} relevant to Sb_2O_4. This indicates the formation of microcrystalline of Sb_2O_4 on catalysts surface because of the interaction between antimony and vanadium. When V_2O_5 loading is lower than 11.2 wt%, Sb_2O_4 microcrystalline and Sb–V mixed oxide co-exist on catalysts surface. When V_2O_5 loading increases to 11.2 wt%, little antimony oxide species exists on catalyst surface so no Raman band of Sb_2O_4 can be observed in the spectrum of $Sb_{20}V_{11.2}O/SiO_2$ catalyst. The relative intensity of the bands relevant to Sb_2O_4 increases with increasing V_2O_5 loading at first and then drops. This suggests that the amount of

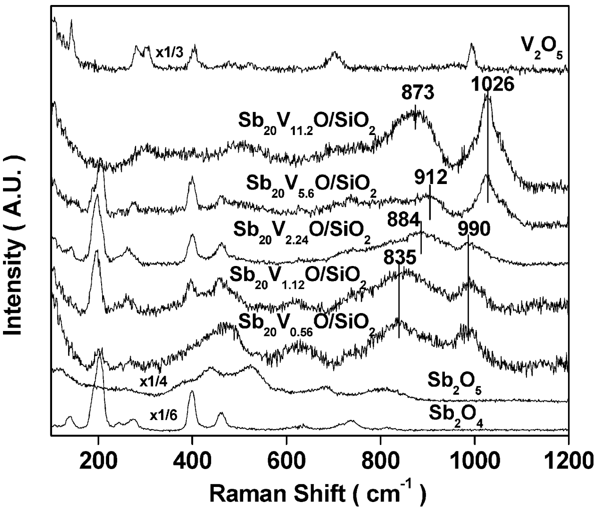

Figure 4. UV Raman spectra of V_2O_5, Sb_2O_4, Sb_2O_5 and $Sb_{20}V_{0.56-11.2}O/SiO_2$ catalysts. $\lambda_{ex} = 325$ nm.

Sb–V mixed oxide on catalysts surface increases with increasing V_2O_5 loading.

The formation of Sb_2O_4 indicates the coexist of Sb^{5+} species and Sb^{3+} species so it is possible to observe the Raman bands for $Sb^{3+}O_X$ species in the spectra of $Sb_{20}V_{0.56-11.2}O/SiO_2$ catalysts. In the spectrum of $Sb_{20}V_{0.56}O/SiO_2$ catalyst, we can see two broad bands at 460 and 608 cm^{-1}, respectively. These two bands are characteristic bands of SiO_2 and highly isolated $Sb^{3+}Ox$ species, respectively. The relative intensity of these two bands decreases with increasing V_2O_5 loading, indicating the increasing amount of Sb–V mixed oxide on catalysts surface. In other researchers' work on bulk Sb–V mixed oxide, it has also been evidenced by XRD that the amount of Sb–V mixed oxide increases with decreasing Sb/V ratio [17]. It was also found that unsupported Sb–V mixed oxide catalysts contained several phases, including Sb–V mixed oxide in rutile phase and Sb_2O_4 [18].

In the spectra of $Sb_{20}V_{0.56-5.6}O/SiO_2$ catalysts, the bands at 835, 884, 912 and 990 cm^{-1} are attributed to Sb–V mixed oxide phase according to very recent reports on Sb–V mixed oxide materials [14,17,19–21]. The bands at 835, 884 and 912 cm^{-1}, which have not been reported previously, are prominent because of resonance enhancement [20,21]. The band at 990 cm^{-1} is assigned to the V = O stretching vibration mode of Sb–V mixed oxide and the bands in the range of 835–912 cm^{-1} are assigned to the Sb–O–V stretching mode of Sb–V mixed oxide phase. In line with the XRD results, the band at 835 cm^{-1} is assigned to the Sb–O–V symmetric stretching mode of Sb_2VO_5 phase and it shifts to 884 cm^{-1} with decreasing Sb/V ratio. The band at 912 cm^{-1} is assigned to the Sb–O–V asymmetric stretching mode of $SbVO_4/VSb_{1-X}O_{4-1.5X}$ phase. In the spectrum of $Sb_{20}V_{5.6}O/SiO_2$ catalyst, a characteristic band of the V = O stretching vibration mode at 1026 cm^{-1} [19,21] can be observed in addition to the band at 912 cm^{-1}, indicating the formation of monomeric VO_4 species on the layer of Sb–V mixed oxide. In the spectrum of $Sb_{20}V_{11.2}O/SiO_2$ catalyst, another band at 873 cm^{-1} appears other than the band at 1026 cm^{-1}. This band at 873 cm^{-1} suggests the formation of polymeric $(VO_3)_n$ species with V–O–V symmetric stretching mode [19,21] on the layer of Sb–V mixed oxide phase. The formation of polymeric $(VO_3)_n$ species on $Sb_{20}V_{11.2}O/SiO_2$ catalyst can explain why the methane conversion for $Sb_{20}V_{11.2}O/SiO_2$ catalyst is higher than that for $Sb_{20}V_{5.6}O/SiO_2$ catalyst.

Although no diffaraction peak can be observed in the XRD patterns of $Sb_{10}V_{0.28-5.6}O/SiO_2$ and $Sb_5V_{0.14-2.8}O/SiO_2$ catalysts, being similar to the analyzing of the Raman spectra of $Sb_{20}V_{0.56-11.2}O/SiO_2$ catalysts, we can obtain the structural information about the Sb–V mixed oxide on $Sb_{10}V_{0.28-5.6}O/SiO_2$ and $Sb_5V_{0.14-2.8}O/SiO_2$ catalysts according to the UV Raman spectra shown in figures 5 and 6. In the Raman spectra of $Sb_5V_{0.14-2.8}O/SiO_2$ and $Sb_{10}V_{0.28-5.6}O/SiO_2$ catalysts, we can see that the relative intensity of the bands relevant to SiO_2 and highly isolated Sb^{3+} oxidic species decreases with increasing V_2O_5 loading but the relative intensity of the bands relevant to Sb–V mixed oxide increases with increasing V_2O_5 loading. This indicates the amount of Sb–V mixed oxide on both $Sb_{10}V_{0.28-5.6}O/SiO_2$ and $Sb_5V_{0.14-2.8}O/SiO_2$ catalysts increases with increasing V_2O_5 loading.

In figure 5, two bands at 835 and 990 cm^{-1} can be observed in the spectra of $Sb_{10}V_{0.28}O/SiO_2$, $Sb_{10}V_{0.56}O/SiO_2$ and $Sb_{10}V_{1.12}O/SiO_2$ catalysts. These two bands indicates the formation of Sb–V mixed oxide in Sb_2VO_5 phase on the surface of these three catalysts. When V_2O_5 loading increases to 2.8 and 5.6 wt%, the band at 835 cm^{-1} shifts to 884 and 912 cm^{-1}, respectively. This shift of Raman band reflects the transform of Sb–V mixed

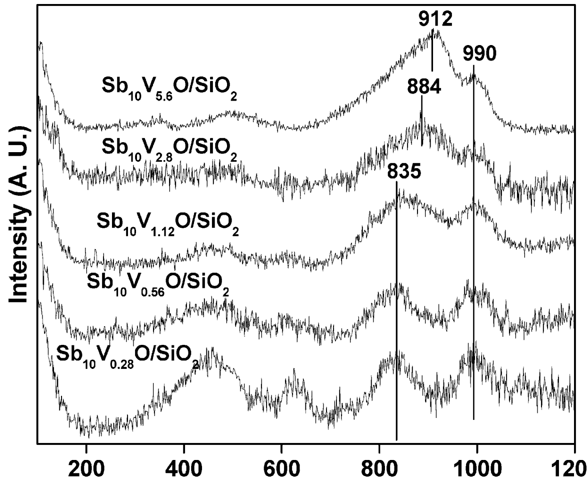

Figure 5. UV Raman spectra of $Sb_{10}V_{0.28-5.6}O/SiO_2$ catalysts. $\lambda_{ex} = 325$ nm.

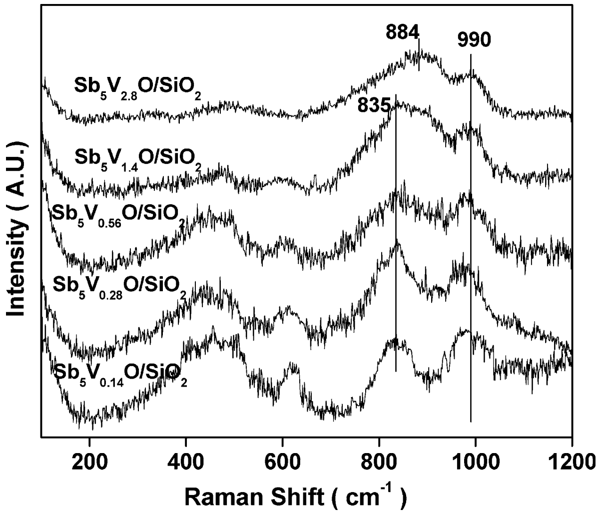

Figure 6. UV Raman spectra of $Sb_5V_{0.14–2.8}O/SiO_2$ catalysts. $\lambda_{ex} = 325$ nm.

oxide from Sb_2VO_5 to $SbVO_4/VSb_{1\text{-}X}O_{4\text{-}1.5X}$ phase as that taking place on $Sb_{20}V_{0.56–11.2}O/SiO_2$ catalysts. The Sb–V mixed oxide on $Sb_{10}V_{2.8}O/SiO_2$ catalyst has a transition structure between Sb_2VO_5 and $SbVO_4/VSb_{1\text{-}X}O_{4\text{-}1.5X}$ phase but the Sb–V mixed oxide on $Sb_{10}V_{5.6}O/SiO_2$ catalyst is in $SbVO_4/VSb_{1\text{-}X}O_{4\text{-}1.5X}$ phase. This can explian why the methane conversion for $Sb_{10}V_{0.28–5.6}O/SiO_2$ catalysts increases with V_2O_5 loading at first but decreases while V_2O_5 loading reaches 5.6 wt%.

In figure 6, two bands at at 835 and 990 cm^{-1} can be observed in the spectra of $Sb_5V_{0.14}O/SiO_2$, $Sb_5V_{0.28}O/SiO_2$, $Sb_5V_{0.56}O/SiO_2$ and $Sb_5V_{1.4}O/SiO_2$ catalysts, indicating the formation of Sb–V mixed oxide in Sb_2VO_5 phase. In the spectrum of $Sb_5V_{2.8}O/SiO_2$ catalyst, the band at 835 cm^{-1} shifts to 884 cm^{-1}. We can know that no Sb–V mixed oxide in $SbVO_4/VSb_{1\text{-}X}O_{4\text{-}1.5X}$ phase but only the Sb–V mixed oxide within a transition structure between Sb_2VO_5 and $SbVO_4/VSb_{1\text{-}X}O_{4\text{-}1.5X}$ phase has formated on $Sb_5V_{2.8}O/SiO_2$ catalyst. This should be the reason why the methane conversion for $Sb_5V_{0.14–2.8}O/SiO_2$ catalysts always increase with V_2O_5 loading as shown in figure 1. The phase transform of Sb–V mixed oxide with decreasing Sb/V ration from Sb_2VO_5 to $SbVO_4/VSb_{1\text{-}X}O_{4\text{-}1.5X}$ phase is less favoured on $Sb_5V_{0.14–2.8}O/SiO_2$ catalysts than on $Sb_{10}V_{0.28–5.6}O/SiO_2$ and $Sb_{20}V_{0.56–11.2}O/SiO_2$ catalysts. This may because the dispersion of Sb–V mixed oxide species on $Sb_5V_{0.14–2.8}O/SiO_2$ catalysts is much better than that on $Sb_{10}V_{0.28–5.6}O/SiO_2$ and $Sb_{20}V_{0.56–11.2}O/SiO_2$ catalysts and so the interaction between Sb–V mixed oxide and silica on $Sb_5V_{0.14–2.8}O/SiO_2$ catalysts is stronger than that on $Sb_{10}V_{0.28–5.6}O/SiO_2$ and $Sb_{20}V_{0.56–11.2}O/SiO_2$ catalysts.

4. Conclusions

In methane selective oxidation with O_2 as oxidant, Sb–V–O/SiO_2 catalysts show the advantages of high activity from VO_X/SiO_2 catalysts as well as high formaldehyde selectivity from SbO_X/SiO_2 catalysts. Higher one-pass formaldehyde yield can be obtained on Sb–V–O/SiO_2 catalysts than on single metal oxide catalysts such as vanadium oxide and antimony oxide catalysts. One-pass formaldehyde yield up to 3% was obtained on Sb–V–O/SiO_2 catalysts at 650 °C. The better catalytic behavior of Sb–V–O/SiO_2 catalysts than that of VO_X/SiO_2 or SbO_X/SiO_2 catalysts results from the formation of Sb–V mixed oxide. A phase transform of Sb–V mixed oxide with decreasing Sb/V ratio from Sb_2VO_5 to $SbVO_4/VSb_{1\text{-}X}O_{4\text{-}1.5X}$ phase takes place on Sb–V–O/SiO_2 catalysts. The Sb–V mixed oxide in Sb_2VO_5 phase is more active and selective in methane selective oxidation than that in $SbVO_4/VSb_{1\text{-}X}O_{4\text{-}1.5X}$ phase.

Acknowledgments

The financial supports from the National Natural Science Foundation of China (NSFC Grant 20273069) and the BP-China project for clean energy facing the future (CEFTF) are acknowledged.

References

[1] R.H. Crabtree, Chem. Rev. 5 (1995) 987.
[2] J.H. Lunsford, Catal. Today 63 (2000) 165.
[3] K. Tabata, Y. Teng, T. Takemoto, E. Suzuki, M. Bañares, M.A. Peña and J.L.G. Fierro, Catal. Rev.-Sci. Eng. 44 (2002) 1.
[4] K. Otsuka and Y. Wang, Appl. Catal. A 222 (2001) 145.
[5] V. Fornés, C. López, H.H. López and A. Martínez, Appl. Catal. A 249 (2003) 345.
[6] X.X. Wang, Y. Wang, Q.H. Tang, Q. Guo, Q.H. Zhang and H. Wan, J. Catal. 217 (2003) 457.
[7] F. Arena, G. Gatti, S. Coluccia, G. Martra and A. Parmaliana, Catal. Today 91–92 (2004) 305.
[8] J.A. Barbero, M.C. Alvarez, M.A. Bañares, M.A. Peña and J.L. Fierro, Chem. Commun. (2002) 1184.
[9] H. Berndt, A. Martin, A. Brückner, E. Schreier, D. Müller, H. Kosslick, G.-U. Wolf and B. Lücke, J. Catal. 191 (2000) 384.
[10] V.D. Sokolovskii, N.J. Coville, A. Parmaliana, I. Eskendirov and M. Makoa, Catal. Today 42 (1998) 191.
[11] A. de Lucas, J.L. Valverde, L. Rodriguez, P. Sanchez and M.T. Garcia, Appl. Catal. A 203 (2000) 81.
[12] T.J. Hall, J.S.J. Hargreaves, G.J. Hutchings, R.W. Joyner and S.H. Taylor, Fuel Proc. Tech. 42 (1995) 151.
[13] A. de Lucas, J.L. Valverde, P. Cañizares and L. Rodrigues, Appl. Catal. A 172 (1998) 165.
[14] M.O.G. Pérez, J.L. Fierro, M.A. Vicente and M.A. Bañares, J. Catal. 206 (2002) 339.
[15] S.J. Miao, L. Liu, Y.X. Lian, X.X. Zhu, S.T. Zhou, Y. Wang and X.H. Bao, Catal. Lett. 97 (2004) 209.
[16] H.D. Zhang, P.L. Ying, J. Zhang, C.H. Liang, Z.C. Feng and C. Li, Stud. Surf. Sci. Catal. 147 (2004) 547.
[17] T. Shishido, A. Inoue, T. Konishi, I. Matsuura and K. Takehira, Catal. Lett. 68 (2000) 215.
[18] H.W. Zanthoff, W. Grünert, S. Buchholz, M. Heber, L. Stievano, F.E. Wagner and G.U. Wolf, J. Mol. Catal. A 162 (2000) 443.
[19] M.A. Bañares and I.E. Wachs, J. Raman Spectr. 33 (2002) 359.
[20] G. Xiong, V.S. Sullivan, P.C. Stair, G.W. Zajac, S.S. Trail, J.A. Kaduk, J.T. Golab and J.F. Brazdil, J. Catal. 230 (2005) 326.
[21] C. Li, J. Catal. 216 (2003) 203.